



NJC

Catalytic Methane Oxidation by Supramolecular Conjugate Based on μ -Nitrido-Bridged Iron Porphyrinoid Dimer

Journal:	<i>New Journal of Chemistry</i>
Manuscript ID	NJ-ART-04-2019-002210.R1
Article Type:	Paper
Date Submitted by the Author:	09-Jun-2019
Complete List of Authors:	Yamada, Yasuyuki; Nagoya University, Research Center for Materials Science Morita, Kentaro; Nagoya University, Department of Chemistry Mihara, Nozomi; Nagoya University, Department of Chemistry Igawa, Kazunobu; Kyushu University, Institute for Materials Chemistry and Engineering Tomooka, Katsuhiko; Kyushu University, Institute for Materials Chemistry and Engineering Tanaka, Kentaro; Nagoya University, Department of Chemistry, Graduate School of Science

SCHOLARONE™
Manuscripts

PAPER

Catalytic Methane Oxidation by Supramolecular Conjugate Based on μ -Nitrido-Bridged Iron Porphyrinoid Dimer

Received 00th January 20xx,
Accepted 00th January 20xx

DOI: 10.1039/x0xx00000x

Yasuyuki Yamada,^{*a,b,c} Kentaro Morita,^b Nozomi Mihara,^b Kazunobu Igawa,^d Katsuhiko Tomooka,^d and Kentaro Tanaka^{*a}

Catalytic methane oxidation was conducted by using a μ -nitrido-bridged dinuclear iron complex of a fourfold rotaxane heterodimer of a porphyrin and a phthalocaynine. Extension of the π -stacked structure of the fourfold rotaxane-based μ -nitrido-bridged iron porphyrinoid dimer by supramolecular complexation with an additional tetraanionic porphyrin apparently increased the methane conversion ability.

Introduction

Methane is the main constituent of natural gas. Following the “shale gas revolution,” significant efforts have been undertaken to develop methods for the direct and efficient conversion of methane into more valuable raw materials such as MeOH, formaldehyde, and formic acid.¹ On the other hand, since methane has a particularly high C-H bond dissociation energy (105 kcal mol⁻¹) among the family of chemically inert light alkanes,² efficient and direct low-temperature C-H activation of methane has been recognized as a long-standing challenge in the field of catalytic chemistry.³⁻⁸

In natural systems, oxygenases such as soluble methane monooxygenase (sMMO), butane monooxygenase, and cytochrome P450 achieve the low-temperature efficient conversion of light alkanes by utilizing high-valent iron-oxo species.⁹⁻¹⁶ These examples have encouraged researchers to produce a variety of biomimetic iron-oxo species and develop a rich research field of iron-oxo-based molecular systems.¹⁷⁻²¹ However, only a few bio-inspired iron-oxo species are capable of oxidizing methane catalytically under mild reaction conditions.^{22, 23} Some iron-oxo species lack oxidizing ability, while others are susceptible to a variety of deactivation reactions, including oxidation of organic ligands and solvents and dimerization to form unreactive species.

Despite these bottlenecks, Sorokin *et al.* found that a μ -nitrido-bridged iron phthalocyanine dimer (**FePc(tBu)₄₂N**) is

capable of oxidizing light alkanes in acidic aqueous solution, in the presence of H₂O₂ at low temperature (< 100 °C).²⁴⁻²⁸ They reported that an ultra-high-valent iron-oxo species, which was generated by the reaction of (**FePc(tBu)₄₂N**) with H₂O₂, was the actual reactive species in this reaction. (**FePc(tBu)₄₂N**) has been recognized as one of the most potent molecular-based methane-oxidation catalysts reported so far.

We recently reported the supramolecular activation of the ethane oxidation activity of a μ -nitrido-bridged dinuclear iron porphyrinoid dimer-based catalyst. For this purpose, we designed a μ -nitrido-bridged dinuclear iron complex constructed in a fourfold rotaxane heterodimer of a porphyrin and a phthalocyanine prepared by using 4,8-diazacyclononyne (DACN) as a terminal stopper (**1⁵⁺·5Cl⁻** in Figure 1). Since **1⁵⁺·5Cl⁻** possesses four peripheral ammonium cations, the addition of an tetraanionic metalloporphyrin (**M-TPPS⁴⁻**, 5,10,15,20-tetrakis(4-sulfonatophenyl)porphyrin metal complex, M = Cu(II) or Ni(II)) resulted in extension of the stacked structure to form **1⁵⁺·M-TPPS⁴⁻·Cl⁻** through π - π stacking and quadruple electrostatic interactions, as shown in Figure 1. The ethane oxidation activity of **1⁵⁺·M-TPPS⁴⁻·Cl⁻** in

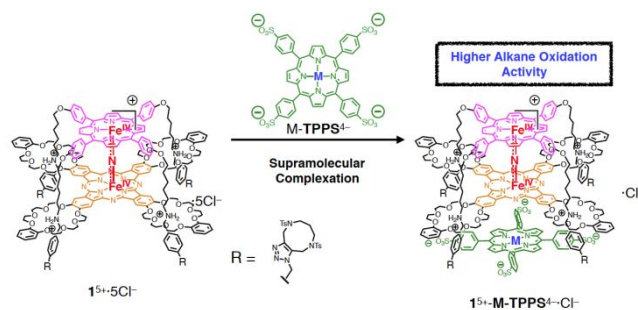


Figure 1. Schematic representation of supramolecular extension of a μ -nitrido-bridged dinuclear iron complex of a fourfold rotaxane heterodimer of a porphyrin and a phthalocyanine **1⁵⁺·5Cl⁻** by complexation with an additional tetraanionic porphyrin **M-TPPS⁴⁻** (M = Cu²⁺ or Ni²⁺).

^a Department of Chemistry, Graduate School of Science, Nagoya University, Furo-cho, Chikusa-ku, Nagoya 464-8602, Japan.

^b Research Center for Materials Science, Nagoya University, Furo-cho, Chikusa-ku, Nagoya 464-8602, Japan.

^c JST, PRESTO, 4-1-8 Honcho, Kawaguchi, Saitama, 332-0012, Japan.

^d Institute for Materials Chemistry and Engineering, and IRCCS, Kyushu University, Kasuga-Koen, Kasuga, Fukuoka, 816-8580, Japan

†E-mail: yy@chem.nagoya-u.ac.jp, kentaro@chem.nagoya-u.ac.jp

Electronic Supplementary Information (ESI) available: [details of any supplementary information available should be included here]. See DOI: 10.1039/x0xx00000x

an acidic aqueous solution, in the presence of H_2O_2 at 60°C , was almost twice that before complexation with **M-TPPS**⁴⁻.²⁹ Thus, **1**⁵⁺-**M-TPPS**⁴⁻-Cl⁻ showed higher catalytic ethane oxidation activity than that of (**FePc**(**tBu**)₄)₂**N**. Herein, we first applied our fourfold rotaxane-based μ -nitrido-bridged iron porphyrinoid dimer to the most difficult light alkane oxidation, that is, the methane oxidation reaction. Moreover, we showed that the catalytic methane oxidation reaction was activated by the supramolecular extension of the π -stacked structure of the fourfold rotaxane-based catalyst.

Results and Discussion

A μ -nitrido-bridged dinuclear iron complex of the fourfold rotaxane heterodimer **1**⁵⁺-5Cl⁻, and its stacked assemblies with **M-TPPS**⁴⁻ (**M** = Cu²⁺: **1**⁵⁺-Cu(II)-TPPS⁴⁻-Cl⁻, **M** = Ni²⁺: **1**⁵⁺-Ni(II)-TPPS⁴⁻-Cl⁻) were synthesized according to our previous report.²⁹ Catalytic methane oxidation reactions using these catalysts were performed in an acidic aqueous solution in the presence of H_2O_2 . H_2O is a suitable solvent for this reaction because the catalysts can decompose most organic solvents, including DMF and CH_3CN .^{2, 24} Since the catalysts were insoluble in H_2O , they were pre-adsorbed on silica gel to prepare solid-supported catalysts. It has already been confirmed by UV-Vis spectroscopy that the stacked structures of **1**⁵⁺ with **M-TPPS**⁴⁻ do not change during adsorption on SiO_2 .²⁹

We first investigated the products of the methane oxidation reaction by **1**⁵⁺-5Cl⁻/ SiO_2 using ¹H NMR spectroscopy. The heterogeneous oxidation of methane was performed using **1**⁵⁺-5Cl⁻/ SiO_2 (141 μM as **1**⁵⁺-5Cl⁻) in D_2O (1.5 mL) containing H_2O_2 (160 mM) and trifluoroacetic acid (TFA, 51 mM) under a methane atmosphere (1.0 MPa) in a 10 mL reaction vessel at 60°C for 8 h. TFA-acidic condition is useful for alkane oxidation by metal ion in the presence of H_2O_2 as well as H_2SO_4 -acidic condition.^{8,30} In this case, acidic condition is necessary for acceleration of the generation of high-valent iron-oxo species by protonation of iron-hydroperoxy species.^{24, 25} The ¹H NMR spectrum of the solution is shown in Figure 2. After the reaction, a signal corresponding to formic acid was observed at 8.26 ppm. The signals at 5.07 and 3.89 were assignable as formaldehyde methyl hemiacetal, whereas signals due

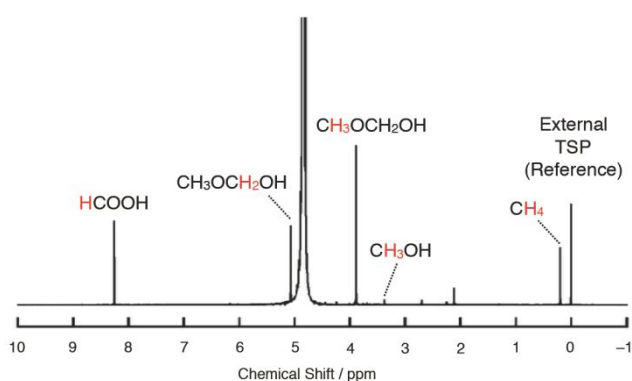


Figure 2. ¹H NMR spectra of the reaction mixture for methane (1.0 MPa) oxidation by **1**⁵⁺-5Cl⁻/ SiO_2 (141 μM as **1**⁵⁺-5Cl⁻) in the presence of H_2O_2 (160 mM) and TFA (51 mM) in D_2O at 60°C for 8 h.

to formaldehyde monohydrate was not observed.^{31,32} This indicated that formaldehyde generated *in situ* reacted with MeOH under the acidic conditions. A very small signal attributed to free MeOH was observed at 3.38 ppm under these conditions. These oxidation reactions did not proceed in the absence of H_2O_2 and were very slow in the absence of TFA. Moreover, these oxidized compounds were formed in apparently smaller amounts or were not observed in the absence of methane, as shown in Figure S1. These results clearly indicated that **1**⁵⁺-5Cl⁻ acted as a methane oxidation catalyst under the present reaction conditions to produce formic acid, formaldehyde, and methanol. Formic acid observed in the absence of methane might be derived from the organic compounds adsorbed on SiO_2 , such as organic solvents. The actual reactive species should be the high-valent iron-oxo complex generated *in situ*,^{24, 27} which we previously observed by electrospray-ionization Fourier transform ion cyclotron resonance mass spectroscopy (ESI-FT-ICR MS).²⁹

Based on these results, we next investigated the time dependence of the concentrations of each product of the catalytic methane oxidation by **1**⁵⁺-5Cl⁻/ SiO_2 . After the reaction in H_2O (1.5 mL) in the presence of **1**⁵⁺-5Cl⁻/ SiO_2 (71 μM), H_2O_2 (160 mM), and trifluoroacetic acid (TFA, 51 mM) under a methane atmosphere (1.0 MPa) in a 10 mL reaction vessel at 60°C , the reaction mixture was analyzed by GC-MS. Formic acid and MeOH were successfully quantified by direct injection of the resulting solution by GC-MS system. MeOH was found to be dissociated from formaldehyde under the GC-MS conditions. However, since direct quantification of formaldehyde was difficult, we derivatized formaldehyde into an *O*-alkyloxime by reaction with *O*-(2,3,4,5,6-pentafluorobenzyl)hydroxylamine (PFBHA) for GC-MS quantification, according to the report by Yu et al.^{33,34}

The results of GC-MS analysis are summarized in Figure 3 and Table S1 (runs 1-10) in the Supporting Information. A gradual increase in the amount of formic acid was observed during the course of the reaction. The concentrations of MeOH and formaldehyde were much lower than that of formic acid even at the initial stage of the reaction (after 1 h). This indicated that the rates of oxidation of MeOH into formaldehyde and formaldehyde into formic acid were much higher than those of methane into MeOH and formic acid into CO_2 . We calculated the total turnover number (TTN_{eff}) and methane conversion number (MCN_{eff}) as indicators of the reaction progress. TTN_{eff} is defined by equations (i) and (ii), where *C* represents the concentration of each species. This is based on the reaction shown in Figure 3(a), where methane was oxidized stepwise into formic acid through MeOH and formaldehyde. On the other hand, MCN_{eff} is defined by equations (iii) and (iv). MCN_{eff} indicates the number of methane molecules converted into MeOH by a single catalyst molecule, whereas TTN_{eff} reflects the number of H_2O_2 molecules consumed by single catalyst molecule for a series of oxidations of methane and its oxidized products. In order to calculate the effective TTN or MCN (TTN_{eff} or MCN_{eff}) for methane oxidation, TTN (MCN) under a N_2 atmosphere was subtracted from that (MCN) under a CH_4 atmosphere.

$$\text{TTN}_{\text{eff}} = \text{TTN}_{(\text{CH}_4)} - \text{TTN}_{(\text{N}_2)} \quad (\text{i})$$

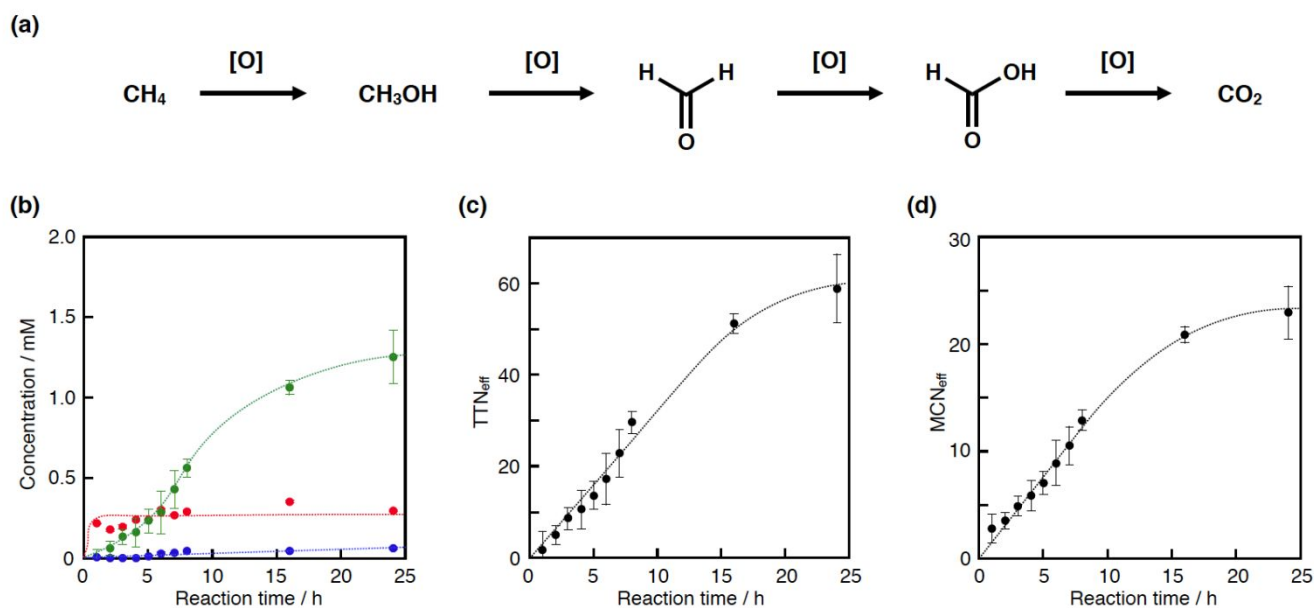


Figure 3. (a) Stepwise methane oxidation reaction by $1^{5+}\text{-5Cl}^-/\text{SiO}_2$. (b) Time dependence of the concentrations of each oxidized product during CH_4 (1.0 MPa) oxidation by $1^{5+}\text{-5Cl}^-/\text{SiO}_2$ in the presence of H_2O_2 (160 mM) and TFA (51 mM) at 60°C (black: methanol, blue: formaldehyde, and red: formic acid). Time dependence of (c) TTN_{eff} and (d) MCN_{eff} for methane oxidation calculated based on the concentration of each product. Error bars indicate standard deviation of three measurements.

$$\text{TTN}_{(\text{CH}_4)} \text{ or } \text{TTN}_{(\text{N}_2)} = (\text{C}_{\text{Methanol}} + 2 \times \text{C}_{\text{Formaldehyde}} + 3 \times \text{C}_{\text{Formic acid}}) / \text{C}_{\text{Cat}} \quad (\text{ii})$$

$$\text{MCN}_{\text{eff}} = \text{MCN}_{(\text{CH}_4)} - \text{MCN}_{(\text{N}_2)} \quad (\text{iii})$$

$$\text{MCN}_{(\text{CH}_4)} \text{ or } \text{MCN}_{(\text{N}_2)} = (\text{C}_{\text{Methanol}} + \text{C}_{\text{Formaldehyde}} + \text{C}_{\text{Formic acid}}) / \text{C}_{\text{Cat}} \quad (\text{iv})$$

TTN_{eff} increased almost linearly up to 8 h, as shown in Figure 3(b), indicating that the catalyst was not degraded and worked stably during this reaction time. However, after 8 h of reaction, TTN_{eff} was saturated. Considering that catalyst degradation hardly occurred for 24 h ethane oxidation under similar reactions, this decrease in the methane oxidation rate was not attributed to catalyst degradation²⁶ but to the overoxidation of formic acid into CO_2 . Although direct observation of the amount of CO_2 generated during the reaction

was difficult, we confirmed that formic acid was gradually oxidized, as shown in Figure S2. This indicated that the oxidizing ability of 1^{5+}-5Cl^- is so strong that even formic acid can be oxidized. Moreover, catalase activity might also contribute to the decrease in catalytic activity by consuming H_2O_2 .³⁵ Furthermore, TTN_{eff} after 8 h of methane oxidation was almost one-fourth of the value for ethane oxidation under the same conditions (Table S1, run 11). This reflected the higher C-H bond dissociation energy of methane compared to that of ethane. Possible reaction mechanism for methane oxidation by 1^{5+} is shown in Figure 4.²⁹ This mechanism is composed of two reaction cycles and the reactive intermediates are the high-valent iron-oxo species **1-c** and **1-d**. In our previous paper, we confirmed that homolytic cleavage of O-O bonding of

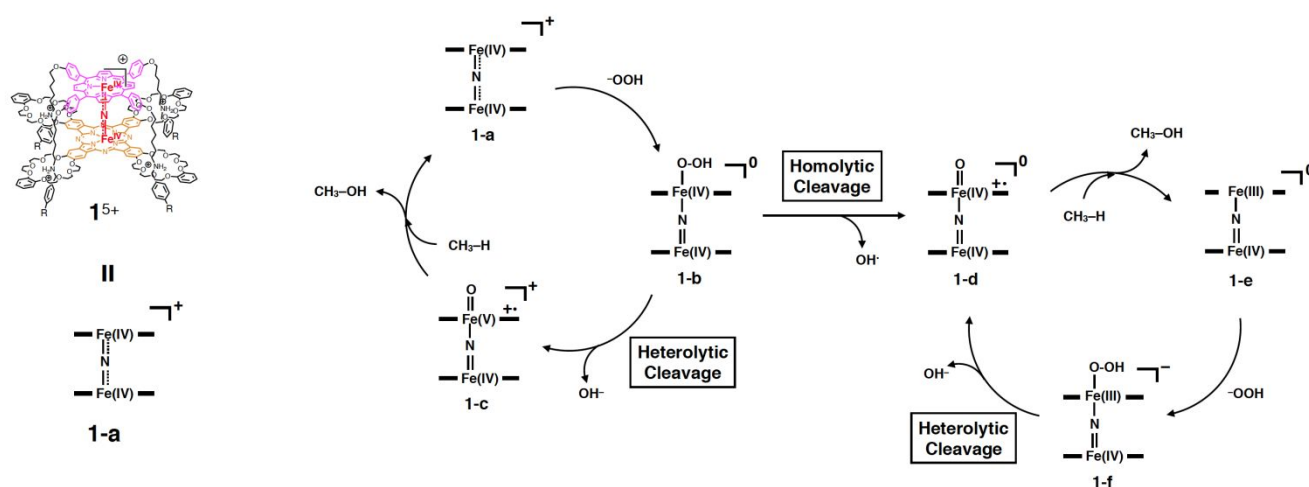


Figure 4. Possible reaction mechanism for methane oxidation by the μ -nitrido-bridged dinuclear iron complex 1^{5+} .

hydroperoxo species (**1-b** to **1-d**) hardly occurred in this reaction condition.²⁹

The methane oxidation ability of supramolecular stacked assemblies (**1⁵⁺-Cu(II)-TPPS⁴⁻-Cl⁻** and **1⁵⁺-Ni(II)-TPPS⁴⁻-Cl⁻**) were examined in the same manner with **1⁵⁺-5Cl⁻** at 60 °C by using the silica-supported catalyst (Figure 5³⁶ and Table S1 (runs 12, 13)). As in the case of **1⁵⁺**, the supramolecular conjugate was stable at least up to 24 h.²⁹ The MCN_{eff} values for **1⁵⁺-Cu(II)-TPPS⁴⁻** and **1⁵⁺-Ni(II)-TPPS⁴⁻** were 18 and 19 after 8 h, which were almost 1.4 times higher than that before complexation. The same trend was observed for TTN_{eff}. The oxo-species of the conjugate should be formed on the iron porphyrin center because **Cu(II)-TPPS⁴⁻** fully covers the iron center of the phthalocyanine unit in **1⁵⁺**.^{37, 38} **1⁵⁺-Ni(II)-TPPS⁴⁻** showed similar reactivity as the **1⁵⁺-Cu(II)-TPPS⁴⁻** conjugate, although **Cu(II)-TPPS⁴⁻** has a spin of *S* = 1/2 while **Ni(II)-TPPS⁴⁻** has no spin (*S* = 0) on its metal center. This suggests that the effect of the central metal ion of TPPS⁴⁻ is not significant despite the close and direct contact of **M-TPPS⁴⁻** with the Fe-N-Fe center of **1⁵⁺**.

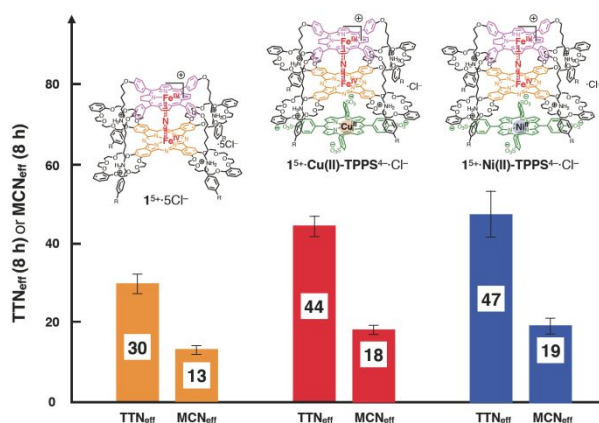


Figure 5. Comparison of MCN_{eff} after 8 h oxidation of methane by μ -nitrido-bridged iron porphyrinoid dimer-based catalyst on silica supports in the presence of H₂O₂ at 60 °C. Error bars indicate standard deviation of three measurements.³⁶

In our previous study on ethane oxidation, we observed a more apparent (almost twofold) enhancement of the catalytic activity after the formation of the stacked assembly with **M-TPPS⁴⁻**.²⁹ We attributed this enhancement to electron donation through the π - π stacking of **1⁵⁺** with **M-TPPS⁴⁻** because the redox potentials of both the 1e⁻ redox waves of Fe(III)/Fe(IV) and π/π^+ showed negative shifts (difference in the redox potentials before and after complexation (ΔE) was up to 0.03 V and 0.02 V, respectively, in CH₂Cl₂ solutions including 0.1 M *n*Bu₄N⁺PF₆⁻). Sorokin reported that a μ -nitrido-bridged phthalocyanine dimer with an electron-donating substituent showed much higher methane oxidizing ability than did that with an electron-withdrawing substituent.²⁵ Moreover, the push effect for the monomeric iron porphyrin is well known, i.e., electron-donating substituents can facilitate the generation of a reactive oxo species by enhancing the liberation of the OH⁻ group from the hydroperoxo-iron species.³⁹⁻⁴² In Figure 4, this liberation of OH⁻ corresponds to the conversion from **1-b** to **1-c** or from **1-f** to **1-g**.

d. However, the degree of enhancement in the case of methane oxidation was significantly lesser than that for ethane oxidation. This difference implies that electron donation by the stacked assembly formation mainly contributes to an increase in the rate of generation of the reactive oxo species (**1-c** or **1-d** in Figure 4), but does not necessarily increase the reactivity of the oxo species.

Conclusions

Herein, we investigated the methane oxidation reaction by utilizing μ -nitrido-bridged iron porphyrinoid dimer-based catalysts constructed in a porphyrin-phthalocyanine heterodimer connected via a fourfold rotaxane structure. Methane was catalytically oxidized into MeOH, formaldehyde, and formic acid in an acidic aqueous solution, in the presence of H₂O₂. Since the fourfold rotaxane heterodimer scaffold has four peripheral ammonium cations, the addition of a tetraanionic porphyrin resulted in close stacking on the phthalocyanine side of the heterodimer. This complexation enhanced the methane oxidation ability of the μ -nitrido-bridged iron porphyrinoid dimer by increasing the generation rate of the reactive oxo species via electron donation through π - π stacking. The findings of this study might contribute to the development of more potent oxidizing catalysts based on iron-oxo species.

Experimental

General

All reagents and solvents were purchased at the highest commercial quality available and used without further purification, unless otherwise stated. The fourfold rotaxane **1⁵⁺-5Cl⁻** and its stacked assemblies with **M-TPPS⁴⁻** (**1⁵⁺-Cu(II)-TPPS⁴⁻-Cl⁻** and **1⁵⁺-Ni(II)-TPPS⁴⁻-Cl⁻**) were prepared according to our previous report.²⁹

Preparation of silica-supported catalysts. Silica-supported catalysts were prepared according to the reported procedure.²⁶ In a typical method, **1⁵⁺-5Cl⁻** (2.81 μ mol) was dissolved in 15 mL of CH₂Cl₂. After the addition of silica gel (473 mg) to the solution, CH₂Cl₂ was evaporated, and the resulting **1⁵⁺-5Cl⁻/SiO₂** was dried under vacuum at 60 °C for 8 h.

¹H NMR analysis of the reaction mixture after CH₄ oxidation by **1⁵⁺-5Cl⁻.** Methane oxidation was performed in a stainless-steel autoclave with a glass tube. A mixture of the catalyst/SiO₂ (211 nmol of Fe complex), TFA (6.0 μ L, 78 μ mol), and 30% H₂O₂ aq. (25 μ L, 245 μ mol) in D₂O (1.5 mL) was heated at 60 °C under 1.0 MPa of methane for 8 h. After the reaction, the mixture was filtrated through a disposable membrane filter, and the filtrate was subjected to NMR analysis using [2,2,3,3,-D₄] sodium 3,3-(trimethylsilyl)propanate (TSP) in D₂O as an external standard. NMR spectra were recorded on a JEOL ECA600 (600 MHz for ¹H) spectrometer at a constant temperature of 298 K.

Methane oxidation reaction. Methane oxidation was performed in a stainless-steel autoclave with a glass tube. A mixture of the catalyst/SiO₂ (106 nmol of Fe complex), TFA (6.0 μ L, 78 μ mol), and 30% H₂O₂ aq. (25 μ L, 245 μ mol) in H₂O (1.5 mL) was heated at 60 °C

under 1.0 MPa of methane for 1–24 h. After the reaction, the mixture was filtrated through a disposable membrane filter, and the resulting filtrate was analyzed by GC-MS (system: Agilent 7890A equipped with JEOL JMS-T100GCV, detection: EI, column: Agilent DB-WAX UI, external standard: isovaleric acid (5 mM), temperature conditions: initial: 70 °C to 220 °C (10 °C/min) – hold (5 min)). The yields of methanol and formic acid were determined based on the results of GC-MS. The yield of formaldehyde was examined using the method reported by Yu et al.^{31,32} Typically, 25 µL of the filtrate obtained from the reaction mixture was diluted with 50 mL of H₂O, followed by the addition of an aqueous solution (469 µM) of PFBOA-HCl (3.0 mL). The resulting mixture was stirred for 2 h. Then, sulfuric acid (1+1) (0.8 mL), NaCl (20 g), and hexane (5.0 mL) were added, and the mixture was stirred vigorously for 5 min. The separated organic layer was dried over anhydrous Na₂SO₄. A mixture of the resulting solution (1.0 mL) and 1.0 mM 1-chlorodecane/hexane solution (10.1 µL) was analyzed by GC-MS.

Conflicts of interest

There are no conflicts to declare.

Acknowledgements

This work was financially supported by a JSPS KAKENHI Grant-in-Aid for Scientific Research (A) (Number 19H00902) to KT, a JSPS KAKENHI Grant-in-Aid for Scientific Research (B) (Number 19H02787), JST PRESTO (Number JK114b), the Shorai Science Foundation for Science and Technology for YY. YY and KI thank to the support by the MEXT project of “Integrated Research Consortium on Chemical Sciences”. We are also grateful to the generous help of Prof. Y. Ohki, Prof. O. Shoji, Dr. S. Ariyasu, and Dr. S. Muratsugu.

Notes and references

- P. C. Bruijninx and B. M. Weckhuysen, *Angew. Chem. Int. Ed.*, 2013, **52**, 11980-11987.
 - S. J. Blansby and G. B. Ellinton, *Acc. Chem. Res.*, 2003, **36**, 255.
 - A. E. Shilov and G. B. Shul'pin, *Chem. Rev.*, 1997, **97**, 2879-2932.
 - C. Copéret, *Chem. Rev.*, 2010, **110**, 656-680.
 - G. B. Shul'pin, *Dalton Trans.*, 2013, **42**, 12794-12818.
 - A. C. Lindhorst, S. Haslinger and F. E. Kuhn, *Chem. Commun.*, 2015, **51**, 17193-17212.
 - D. S. Nesterov, O. V. Nesterova and A. J. L. Pombeiro, *Coord. Chem. Rev.*, 2018, **355**, 199-222.
 - M. Ravi, M. Ranocchiari and J. A. van Bokhoven, *Angew. Chem. Int. Ed.*, 2017, **56**, 16464-16483.
 - M. Bordeaux, A. Galarneau and J. Drone, *Angew. Chem. Int. Ed.*, 2012, **51**, 10712-10723.
 - T. J. Lawton and A. C. Rosenzweig, *J. Am. Chem. Soc.*, 2016, **138**, 9327-9340.
 - A. Trehoux, J.-P. Mahy and F. Avenier, *Coord. Chem. Rev.*, 2016, **322**, 142-158.
 - V. C. Wang, S. Maji, P. P. Chen, H. K. Lee, S. S. Yu and S. I. Chan, *Chem. Rev.*, 2017, **117**, 8574-8621.
 - K. S. Rabe, V. J. Gandubert, M. Spengler, M. Erkelenz and C. M. Niemeyer, *Anal. Bioanal. Chem.*, 2008, **392**, 1059-1073.
 - M. Sono, M. P. Roach, E. D. Coulter and J. H. Dawson, *Chem. Rev.*, 1996, **96**, 2841-2887.
 - A. R. McDonald and L. Que, *Coord. Chem. Rev.*, 2013, **257**, 414-428.
 - W. Nam, *Acc. Chem. Res.*, 2007, **40**, 522-531.
 - H. Fujii, *Coord. Chem. Rev.*, 2002, **226**, 51-60.
 - A. Gunay and K. H. Theopold, *Chem. Rev.*, 2010, **110**, 1060-1081.
 - A. B. Sorokin, *Chem. Rev.*, 2013, **113**, 8152-8191.
 - E. P. Talsi and K. P. Bryliakov, *Coord. Chem. Rev.*, 2012, **256**, 1418-1434.
 - C. W. Tse, T. W. Chow, Z. Guo, H. K. Lee, J. S. Huang and C. M. Che, *Angew. Chem. Int. Ed.*, 2014, **53**, 798-803.
 - G. V. Nizova, B. Krebs, G. Süß-Fink, S. Schindler, L. Westerheide, L. G. Cuervoc and G. B. Shul'pin, *Tetrahedron*, 2002, **58**, 9231-9237.
 - S. I. Chan, Y. J. Lu, P. Nagababu, S. Maji, M. C. Hung, M. M. Lee, I. J. Hsu, P. D. Minh, J. C. Lai, K. Y. Ng, S. Ramalingam, S. S. Yu and M. K. Chan, *Angew. Chem. Int. Ed.*, 2013, **52**, 3731-3735.
 - A. B. Sorokin, E. V. Kudrik and D. Bouchu, *Chem. Commun.*, 2008, **0**, 2562-2564.
 - P. Afanasiev and A. B. Sorokin, *Acc. Chem. Res.*, 2016, **49**, 583-593.
 - L. X. Alvarez and A. B. Sorokin, *J. Organomet. Chem.*, 2015, **793**, 139-144.
 - E. V. Kudrik, P. Afanasiev, L. X. Alvarez, P. Dubourdeaux, M. Clemancey, J. M. Latour, G. Blondin, D. Bouchu, F. Albrieux, S. E. Nefedov and A. B. Sorokin, *Nat. Chem.*, 2012, **4**, 1024-1029.
 - M. G. Quesne, D. Senthilnathan, D. Singh, D. Kumar, P. Maldivi, A. B. Sorokin and S. P. de Visser, *ACS Catalysis*, 2016, **6**, 2230-2243.
 - N. Mihara, Y. Yamada, H. Takaya, Y. Kitagawa, K. Igawa, K. Tomooka, H. Fujii and K. Tanaka, *Chem. Eur. J.*, 2019, **25**, 3369-3375.
 - L. C. Kao, A. C. Hutson and A. Sen, *J. Am. Chem. Soc.*, 1991, **113**, 700-701.
 - S. Morooka, C. Wakai, N. Matsubayasi and M. Nakahara, *J. Phys. Chem. A*, 2005, **109**, 6610-6619.
 - V. M. Nosova, Y. A. Ustynyuk, L. G. Bruk, O. N. Temkin, A. V. Kisin and P. A. Storozhenko, *Inorg. Chem.*, 2011, **50**, 9300-9310.
 - S. Ho, S. H. and J. Z. Yu, *Anal. Chem.*, 2002, **74**, 1232-1240.
 - X. Pang and A. C. Lewis, *Anal. Methods*, 2012, **4**.
 - M. F. Zippies, W. A. Lee and T. C. Bruce, *J. Am. Chem. Soc.*, 1986, **108**, 4433-4445.
- Considering that TTN and MCN for methane oxidation started to decrease especially after 16 hours reaction, we decided to compare TTN and MCN values at 8 hours reaction.
- Y. Yamada, N. Mihara, S. Shibano, K. Sugimoto and K. Tanaka, *J. Am. Chem. Soc.*, 2013, **135**, 11505-11508.
 - N. Mihara, Y. Yamada, S. Akine, K. Sugimoto and K. Tanaka, *Chem. Commun.*, 2017, **53**, 2230-2232.
 - K. Yamaguchi, K. Watanabe and I. Morishima, *Inorg. Chem.*, 1992, **31**, 156-157.

ARTICLE

Journal Name

- 1
2
3 40 K. Yamaguchi, Y. Watanabe and I. Morishima, *J. Chem. Soc., Chem. Commun.*, 1992, **0**, 1709-1710.
4
5 41 K. Watanabe, in *High-Valent Intermediates*, eds. K. M. Kadish, K. M. Smith and R. Guilard, Elsevier, 2003, vol. 4,
6 ch. 30.
7 42 S. Yokota and H. Fujii, *J. Am. Chem. Soc.*, 2018, **140**, 5127-
8 5137.
9
10
11
12
13
14
15
16
17
18
19
20
21
22
23
24
25
26
27
28
29
30
31
32
33
34
35
36
37
38
39
40
41
42
43
44
45
46
47
48
49
50
51
52
53
54
55
56
57
58
59
60

Table of Content

Catalytic CH₄ oxidation by μ -nitrido-bridged iron porphyrinoid dimer was successfully activated by supramolecular complexation.

